JACS
JOURNAL OF THE AMERICAN CHEMICAL SOCIETY

Communication

pubs.acs.org/JACS

Dibenzothiopheno[6,5-*b*:6′,5′-*f*]thieno[3,2-*b*]thiophene (DBTTT): High-Performance Small-Molecule Organic Semiconductor for Field-Effect Transistors

Jeong-Il Park,*[,†,∥] Jong Won Chung,[†,∥] Joo-Young Kim,[†] Jiyoul Lee,[†,§] Ji Young Jung,[†] Bonwon Koo,[†] Bang-Lin Lee,[†] Soon W. Lee,[‡] Yong Wan Jin,[†] and Sang Yoon Lee[†]

[†]Material Research Center, Samsung Advanced Institute of Technology, Samsung Electronics Co., Ltd., Samsung-ro 130, Yongtong-gu, Suwon-si, Gyeonggi-do 443-803, Korea

[‡]Department of Chemistry, Sungkyunkwan University Natural Science Campus, Seobu-ro 2066, Jangan-gu, Suwon-si, Gyeonggi-do 440-746, Korea

[§]Department of Graphic Arts Information Engineering, College of Engineering, Pukyong National University, 365 Sinseron-ro, Nam-gu, Busan 608-739, Korea

Supporting Information

ABSTRACT: We present the synthesis, characterization, and structural analysis of a thiophene-rich heteroacene, dibenzothiopheno[6,5-*b*:6′,5′-*f*]thieno[3,2-*b*]thiophene (DBTTT) as well as its application in field-effect transistors. The design of DBTTT is based on the enhancement of intermolecular charge transfer through strong S−S interactions. Crystal structure analysis showed that the intermolecular $\pi-\pi$ distance is shortened and that the packing density is higher than those of the electronically equivalent benzene analogue, dinaphtho-[2,3-*b*:2′,3′-*f*]thieno[3,2-*b*]thiophene (DNTT). The highest hole mobility we obtained in polycrystalline DBTTT thin-film transistors was 19.3 $cm^2 \cdot V^{-1} \cdot s^{-1}$, six times higher than that of DNTT-based transistors. The observed isotropic angular mobilities and thermal stabilities at temperatures up to 140 °C indicate the great potential of DBTTT for attaining device uniformity and processability.

Organic semiconductors are drawing attention as promising materials that can be applied in flexible electronics, despite their relatively low charge mobility when compared to their inorganic counterparts.[1,2] New materials with high mobilities above 10 $cm^2 \cdot V^{-1} \cdot s^{-1}$ and recently developed sophisticated solution-processing techniques for single-crystalline devices have spurred many researchers to develop organic semiconductors for next-generation flexible electronics.[3−6]

Heteroacenes that contain chalcogenophene have been actively investigated as semiconducting materials because they are more stable in air than acenes and various chemical modifications of the compounds are possible.[7,8] While there have been many attempts to combine benzene with thiophene rings to produce higher-performance materials, only a few derivatives are known to show high mobilities above 1 $cm^2 \cdot V^{-1} \cdot s^{-1}$. Diacene-fused thieno-[3,2-*b*]thiophenes (DNTTs)[9] have been studied in depth by many researchers to demonstrate their applicability in new-concept devices because of their high mobility.[10−12] For further enhancement of the mobility of DNTT, Takimiya[13] and Bao[14] et al. introduced anthracene instead of naphthalene to facilitate the charge transfer between molecules by increasing the $\pi-\pi$ orbital overlap; however, the resulting TFT performance did not surpass that of TFTs based on unmodified DNTT. While there are some examples of the mobility being enhanced by side-chain modifications of DNTT,[15−20] we focused on developing new core molecules with high performance. Although theoretical simulations suggest that the highly symmetric benzene ring is more favorable than the thiophene ring for low reorganization energy and charge transfer is dependent on the conjugation length of the molecule, we focused on the compactness of molecules for a higher density of charge-carrying species and introducing strong S−S and S−C interactions between thiophenes instead of the C−H···π interactions through benzene rings.

By replacing the terminal benzene rings of DNTT with two thiophene rings, as shown in Figure 1, we propose a four-

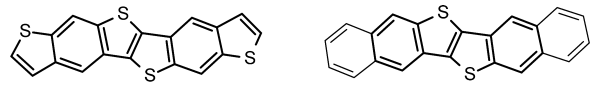

Figure 1. Chemical structure of DBTTT and DNTT.

thiophene-fused heteroacene, dibenzothiopheno[6,5-*b*:6′,5′-*f*]-thieno[3,2-*b*]thiophene (DBTTT), as a candidate for a higher-charge-transporting material. Owing to the higher number of thiophenes, DBTTT has a lower HOMO level and a larger HOMO−LUMO energy gap than DNTT in molecular orbital calculation (HOMO, highest occupied molecular orbital; LUMO, lowest unoccupied molecular orbital). Calculations show that the reorganization energy of DBTTT (146 meV) is comparable to that of DNTT (128 meV). In addition, crystal-structure prediction using the Polymorph package in Materials Studio (BIOVIA, formerly Accelrys, USA) shows that, compared to DNTT, DBTTT molecules are more closely packed and that

Received: February 10, 2015
Published: March 31, 2015

DOI: 10.1021/jacs.5b01108
J. Am. Chem. Soc. 2015, 137, 12175−12178

the packing density is over 10% higher (see Supporting Information). We report here its synthesis, physicochemical properties, crystal structure, and thin-film and single-crystalline transistor characteristics to examine the suitability of DBTTT as a high-performance semiconducting material.

In our study, DBTTT was regiospecifically synthesized by adapting Neckers' method,[21] where dilithiated thieno[3,2-*b*]thiophene was condensed with 3-bromo-thiophene-2-carboxaldehyde and by in situ dehydroxylation using sodium cyanoborohydride to afford compound **3** in Scheme 1. Using a

Scheme 1. Synthetic Route to DBTTT

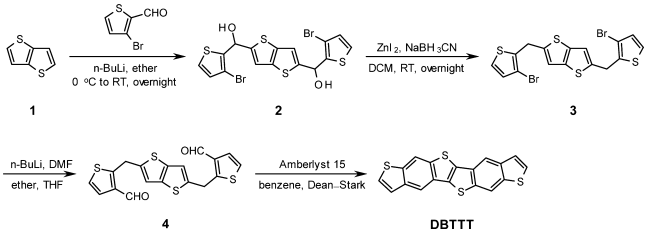

little excess of *tert*-butyllithium (*t*-BuLi) and dimethylformamide (DMF), the dibromo compound was converted to dicarboxaldehyde, compound **4**, with good yield (42% in three steps). The tandem intramolecular cyclodehydration (hetero-Bradsher reaction) afforded the final product as an off-white solid, which was further purified by sublimation.

DBTTT is a thermally stable pale-yellow crystal that sublimes at temperatures above 350 °C (T_m = 427 °C). The optical HOMO−LUMO gap estimated from the absorption edge (λ_{edge} = 423 nm) is about 2.9 eV, which is similar to that of DNTT (3.0 eV). The ionization potential for DBTTT is 5.32 eV below the vacuum level. Judging from this data, we expect DBTTT to be electrochemically as stable as DNTT.

Single-crystal X-ray analysis of DBTTT elucidated that the compound exhibited a typical herringbone packing structure with a small standard deviation of 0.04 Å. Compared to the well-known DNTT, the intermolecular distance between two adjacent DBTTT molecules along the π-stacking direction was dramatically reduced to 5.91 Å (6.19 Å for DNTT), and all sulfur atoms participated in the sulfur−sulfur van der Waals interaction on the *a*−*b* plane and even along the *c*-axis. Unlike other high-performance semiconducting materials like DNTT, pentacene, or rubrene, the transfer integral values[22] of DBTTT on the *a*−*b* plane were quite well balanced (V_{T1} = 67, V_{T2} = 50, and V_{TP} = 70 meV). The Marcus-theory-based[23] directional charge mobilities of DBTTT ranged from 2.5 to 5.6 $cm^2 \cdot V^{-1} \cdot s^{-1}$. Compared to the structurally similar DNTT and dianthra[2,3-*b*:2′,3′-*f*]thieno[3,2-*b*]thiophene (DATT) crystals, the transfer integral values were quite distinguishable (Figure 2d), and the calculated ratio between the maximum and minimum angular mobility, μ_{max}/μ_{min}, of DBTTT was much lower than those of DNTT and DATT (9.3/2.9 and 15.5/5.2, respectively). It is noteworthy that, even though the maximum and average mobilities of DBTTT are expected to be lower, the isotropic mobility of DBTTT can be evaluated in polycrystalline thin films because anisotropic charge transport may obstruct the prediction of the characteristics and complicate circuit and device design. Furthermore, the grain boundary of isotropic microcrystals probably reduces the energy barrier to transport and possibly contribute to the improvement in device uniformity.

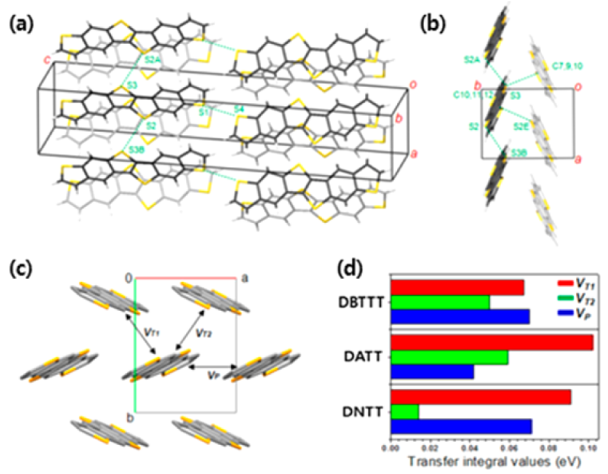

Figure 2. Crystal structure and transfer integral value of DBTTT. (a,b) There are two kinds of intermolecular S···S contacts (S1−S4, S2−S3) that are shorter than the sum of van der Waals radius of the sulfur atoms (3.70 Å). (c) *c*-Axis projection representing the herringbone structure. The transfer integrals were computed for the transverse (V_{T1} and V_{T2}) and parallel (V_{TP}) components of pairs of nearest neighbors. H atoms have been omitted for clarity. (d) Comparison of transfer integral values of DBTTT with those of other thienothiophene-cored organic semiconductors, DNTT and DATT.

Thin-film transistors were fabricated by vacuum deposition on the octadecyltrichlorosilane (ODTS)-treated SiO_2/Si (300 nm-thick thermal SiO_2 on Si wafer) substrates. The channel width and length of the DBTTT were 1000 and 100 μm, respectively. Table 1 summarizes the performance of the DBTTT-based

Table 1. Experimental Characteristics of DBTTT-Based Organic Field-Effect Transistors (OFETs)

substrate temp (°C)	mobility[a] ($cm^2 \cdot V^{-1} \cdot s^{-1}$)	I_{on}/I_{off}	threshold voltage (V)
RT	2.82 ± 0.71	10^6−10^7	− 7.91 ± 2.34
40	6.89 ± 0.84	10^7	− 8.32 ± 1.14
60	13.87 ± 2.34	10^8	− 9.82 ± 2.75
80	8.26 ± 1.15	10^7	− 9.76 ± 0.75

[a]Extracted from saturation regime (V_{DS} = −40 V).

organic field-effect transistors (OFETs) prepared at various substrate temperatures (T_{sub}). All the devices showed typical p-channel field-effect transistor (FET) characteristics. In particular, excellent FET characteristics, with average mobility of μ_{FET} = 13.9 ± 2.3 $cm^2 \cdot V^{-1} \cdot s^{-1}$ and on/off current ratio of $I_{on}/I_{off} > 10^7$ were obtained from 36 devices fabricated at T_{sub} = 60 °C. Among the results, the highest hole mobility of 19.3 $cm^2 \cdot V^{-1} \cdot s^{-1}$ was achieved with a threshold voltage (V_{th}) of −11.2 V in the saturation region. The value of I_{on}/I_{off} was around 3.6×10^8. The mobility is the highest value ever reported among polycrystalline thin-film transistors fabricated on SiO_2/Si substrates. The output characteristics (drain current, I_D, versus drain−source bias, V_{DS}) and transfer characteristics (I_D versus gate−source bias, V_{GS}) of the devices are shown in Figure 3.

The substrate temperature influenced the crystalline domain sizes, as shown in the atomic force microscopy (AFM) images (Figure 4a). The grains were ∼0.1 μm in size in the thin films deposited at room temperature (RT), whereas the grain sizes were 1−2 μm in the films deposited at T_{sub} = 60 °C. Apparently, the larger grains contributed to the enhancement in hole

DOI: 10.1021/jacs.5b01108
J. Am. Chem. Soc. 2015, 137, 12175−12178

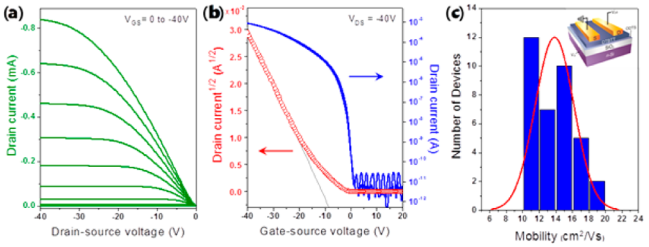

Figure 3. Device performance of DBTTT-based OFETs. (a) Output characteristics (I_D versus V_{DS}) and (b) transfer characteristics (I_D versus V_{GS}) of DBTTT-based OFETs fabricated on ODTS-treated SiO_2/Si substrate with a width/length ratio of 10. (c) Histogram of the mobilities obtained from 36 devices. The inset image shows the device structure with top contact and bottom gate.

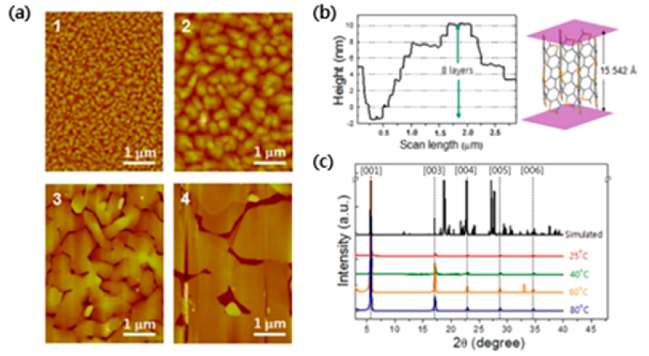

Figure 4. AFM image and XRD patterns obtained at different substrate temperatures. (a) AFM images of the evaporated thin films deposited on ODTS-treated SiO_2/Si substrates at T_{sub} of (1) 25, (2) 40, (3) 60, and (4) 80 °C. Scale bar: 1 μm. (b) Cross-sectional profile of (a3). (c) Out-of-plane XRD patterns of DBTTT on ODTS-modified substrates at different substrate temperatures (black line, simulated from single crystallographic data; red line, T_{sub} = 25 °C; green line, T_{sub} = 40 °C; orange line, T_{sub} = 60 °C; blue line, T_{sub} = 80 °C). The *d*-spacing of the evaporated DBTTT film, obtained from the reflection peak, was 15.5 Å.

mobility.[24] When DBTTT was deposited at a higher temperature (80 °C), larger, albeit noncontinuous, crystallites were observed, which is consistent with the weaker field-effect response in actual devices.

The X-ray diffraction (XRD) patterns of the DBTTT thin films show well-defined crystalline character, and the peaks are clearly assignable to (001) reflections (Figure 4c). A primary diffraction peak appears at $2\theta = 5.68°$, with third- to sixth-order diffraction peaks at 2θ = 17.10, 22.86, 28.66, and 34.58°, respectively. The strong intensity of the XRD peaks indicates the formation of lamellar ordering, and the crystallinity of the substrate. The *d*-spacing of DBTTT obtained from the first reflection peak was 15.5 Å, which is consistent with the single-layer thickness obtained by AFM (Figure 4b). As shown in the AFM images (Figure 4a,b), the molecules stood almost perpendicular to the substrate surface and the packing nature of the microcrystal in the thin film was similar to that of the solution-grown single crystal.

To confirm the intrinsic mobility of DBTTT, single-crystalline field-effect transistors (SC-FETs) were fabricated. Using the physical vapor transport (PVT) method,[25] the crystals were directly grown on a SiO_2/Si substrate coated with a self-assembled monolayer (SAM) of ODTS. The micrometer-sized single-crystalline plates, as large as 20 × 20 ± 5 μm with a typical thickness of ~40 ± 2 nm, were obtained with a regular hexagonal shape, where the angles of the facets match those calculated from the X-ray structure (Figure 2a,b). The SC-FETs were fabricated using the "organic ribbon mask" technique[26] in which an individual organic ribbon was used as a mask for the deposition of gold for the source and drain electrodes. Top-contact bottom-gate devices were produced (Figure 5c). The angular depend-

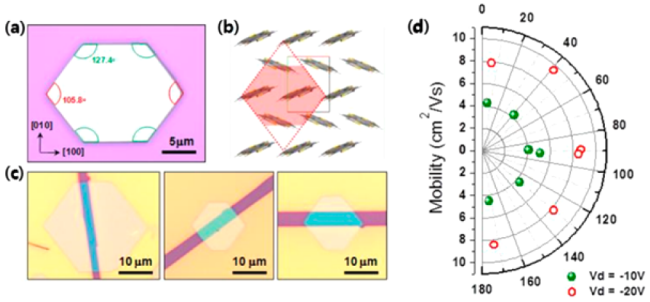

Figure 5. Highly regular hexagonal crystal and electrical characteristics of single-crystalline FETs along different crystal planes. (a) Optical microscope image of the hexagonal crystal with the facets indexed. (b) Herringbone arrangement of the molecules when viewed along the *c*-axis. (c) Optical microscope image of DBTTT transistors consisting of individual single crystals with different channel directions. Carrier transport along the (left) [100], (center) [110], and (right) [010] directions. (d) Experimental results of the channel-direction-dependent charge-carrier mobility in the range of 0−180° (V_{GS} = −40 V; V_{DS} = −10 V, −20 V).

ence of the field-effect mobility of DBTTT appeared quite uniform, regardless of the channel direction. As shown in Figure 5d, the transistors exhibited very similar mobilities of about 4.06−5.11 $cm^2 \cdot V^{-1} \cdot s^{-1}$ along the [100], [110], and [010] directions. As the gate bias increased, the saturation mobility increased to 8.53 ± 0.56 $cm^2 \cdot V^{-1} \cdot s^{-1}$ (V_{DS} at −20 V). With further increase of the bias to −40 V, some devices underwent breakage, although the saturation mobility was observed to be 18.0 $cm^2 \cdot V^{-1} \cdot s^{-1}$.

In order to evaluate the thermal stability of DBTTT-based FET devices, the temperature-dependent electrical characteristics were measured by elevating the temperature from RT to 200 °C in steps of 10 °C. The transfer characteristics, mobility, and V_{th} remained at their initial values until the temperature reached 140 °C (Figure 6). Although a 50% decrease in mobility and negative shift of V_{th} were observed when the temperature exceeded 150 °C, the mobility was restored to the initial value after cooling to RT. Compared to its benzene analogue, DNTT, the improved thermal stability of DBTTT can be explained by

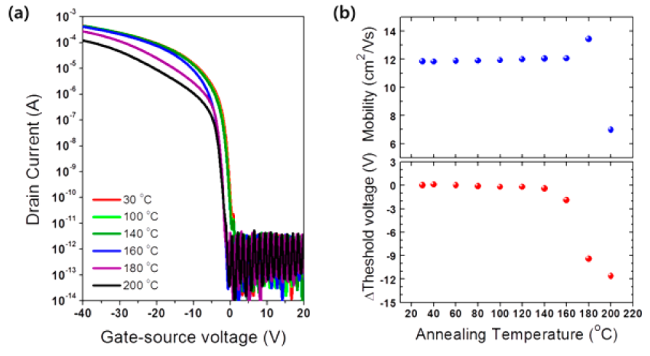

Figure 6. (a) Transfer curves and (b) mobility and V_{th} of DBTTT at different temperatures.

DOI: 10.1021/jacs.5b01108
J. Am. Chem. Soc. 2015, 137, 12175−12178

the stiffness of the packing structure of DBTTT owing to multiple S···S contacts and closer $\pi-\pi$ distance, resulting in higher packing density (1.473 g·cm^{-3} for DNTT; 1.622 g·cm^{-3} for DBTTT).

We have designed and efficiently synthesized a novel organic semiconductor with thermal stability and durability. The high-performance transistor characteristics originated from the unique interaction between DBTTT molecules owing to the additional thiophenes, resulting in closer contact in the crystal lattice. In addition to the strong $\pi-\pi$ stacking interaction, the intermolecular networking in the crystal lattice through S···S van der Waals contacts dramatically enhanced the charge-carrying mobility to 19.3 cm^2·V^{-1}·s^{-1} in a polycrystalline thin-film transistor. The isotropic charge-transfer characteristics of single-crystalline FETs are considered an additional benefit for facilitating charge transfer in multigrain thin films.[27,28] Based on these results, we conclude that DBTTT can be a very promising candidate for practical application in future organic electronics.

■ ASSOCIATED CONTENT

Supporting Information

Experimental details, synthesis, characterization, device fabrication, theoretical studies, and crystal data. This material is available free of charge via the Internet at http://pubs.acs.org.

■ AUTHOR INFORMATION

Corresponding Author

*jeong.park@samsung.com

Author Contributions

‖J.P. and J.W.C. contributed equally to the manuscript.

Notes

The authors declare no competing financial interest.

■ ACKNOWLEDGMENTS

The authors gratefully acknowledge W. Hu (ICCAS) for supporting the fabrication of SC-FET devices, K. E. Lee (SKKU) for her assistance with the work on X-ray single crystallography, A. Aspuru-Guzik (Harvard University) for providing DATT crystal structure files, and Z. Bao (Stanford University) for useful discussions. This work was supported in part by the Global Leading Technology Program funded by the Ministry of Trade, Industry, and Energy, Republic of Korea. (10042419).

■ REFERENCES

(1) Gelinck, G.; Heremans, P.; Nomoto, K.; Anthopoulos, T. D. *Adv. Mater.* **2010**, *22*, 3778.

(2) Di, C.; Zhang, F.; Zhu, D. *Adv. Mater.* **2013**, *25*, 313.

(3) Minemawari, H.; Yamada, T.; Matsui, H.; Tsutsumi, J.; Haas, S.; Chiba, R.; Kumai, R.; Hasegawa, T. *Nature* **2011**, *475*, 364.

(4) Giri, G.; Verploegen, E.; Mannsfeld, S.; Atahan-Evrenk, S.; Kim, D. H.; Lee, S. Y.; Becerril, H. A.; Aspuru-Guzik, A.; Toney, M. F.; Bao, Z. *Nature* **2011**, *480*, 504.

(5) Yuan, Y.; Giri, G.; Ayzner, A. L.; Zoombelt, A. P.; Mannsfeld, C. B.; Chen, J.; Nordlund, D.; Toney, M. F.; Huang, J.; Bao, Z. *Nat. Commun.* **2014**, *5*, 3005.

(6) Mitsui, C.; Okamoto, T.; Yamagishi, M.; Tsurumi, J.; Yoshimoto, K.; Nakahara, K.; Soeda, J.; Hirose, Y.; Sato, H.; Yamano, A.; Uemura, T.; Takeya, J. *Adv. Mater.* **2014**, *26*, 4546.

(7) Takimiya, K.; Shinamura, S.; Osaka, I.; Miyazaki, E. *Adv. Mater.* **2011**, *23*, 4347.

(8) Takimiya, K.; Osaka, I.; Mori, T.; Nakano, M. *Acc. Chem. Res.* **2014**, *47*, 1493.

(9) Yamamoto, T.; Takimiya, K. J. *Am. Chem. Soc.* **2007**, *129*, 2224.

(10) Zschieschang, U.; Ante, F.; Kalblein, D.; Yamamoto, T.; Takimiya, K.; Kuwabara, H.; Ikeda, M.; Sekitani, T.; Someya, T.; Blochwitz-Nimoth, J.; Klauk, H. *Org. Electron.* **2011**, *12*, 1370−1375.

(11) Kuribara, K.; Wang, H.; Uchiyama, N.; Fukuda, K.; Yokota, T.; Zschieschang, U.; Jaye, C.; Fischer, D.; Klauk, H.; Yamamoto, T.; Takimiya, K.; Ikeda, M.; Kuwabara, H.; Sekitani, T.; Loo, Y.-L.; Someya, T. *Nat. Commun.* **2012**, *3*, 723.

(12) Ante, F.; Kalblein, D.; Zschieschang, U.; Canzler, T. W.; Werner, A.; Takimiya, K.; Ikeda, M.; Sekitani, T.; Someya, T.; Klauk, H. *Small* **2011**, *7*, 1186.

(13) Niimi, K.; Shinamura, S.; Osaka, I.; Miyazaki, E.; Takimiya, K. *J. Am. Chem. Soc.* **2011**, *133*, 8732.

(14) Sokolov, A. N.; Atahan-Evrenk, S.; Mondal, R.; Akkerman, H. B.; Sanchez-Carrera, R. S.; Granados-Focil, S.; Schrier, J.; Mannsfeld, C. B.; Zoombelt, A. P.; Bao, Z.; Aspuru-Guzik, A. *Nat. Commun.* **2011**, *2*, 437.

(15) Kang, M. J.; Doi, I.; Mori, H.; Miyazaki, E.; Takimiya, K.; Ikeda, M.; Kuwabara, H. *Adv. Mater.* **2011**, *23*, 1222.

(16) Niimi, K.; Kang, M. J.; Miyazaki, E.; Osaka, I.; Takimiya, K. *Org. Lett.* **2011**, *13*, 3430.

(17) Hofmockel, R.; Zschieschang, U.; Kraft, U.; Rődel, R.; Hansen, N. H.; Stolte, M.; Wűrthner, F.; Takimiya, K.; Kern, K.; Pflaum, J.; Klauk, H. *Org. Electron.* **2013**, *14*, 3213.

(18) Matsumoto, T.; Ou-Yang, W.; Miyake, K.; Uemura, T.; Takeya, J. *Org. Electron.* **2013**, *14*, 2590.

(19) Yokota, T.; Kuribara, K.; Tokuhara, T.; Zschieschang, U.; Klauk, H.; Takimiya, K.; Sadamitsu, Y.; Hamada, M.; Sekitani, T.; Someya, T. *Adv. Mater.* **2013**, *25*, 3639.

(20) Amin, A. Y.; Khassanov, A.; Reuter, K.; Meyer-Friedrichsen, T.; Halik, M. *J. Am. Chem. Soc.* **2012**, *134*, 16548.

(21) Wex, B.; Kaafarani, B. R.; Kirschbaum, K.; Neckers, D. C. *J. Org. Chem.* **2005**, *70*, 4502.

(22) *ADF2008.01*; SCM, Theoretical Chemistry, Vrije Universiteit: Amsterdam, The Netherlands. http://www.scm.com (accessed Oct. 14, 2014).

(23) Marcus, R. A. *Angew. Chem., Int. Ed.* **1993**, *32*, 1111.

(24) Headrick, R. L.; Wo, S.; Sansoz, F.; Anthony, J. E. *Appl. Phys. Lett.* **2008**, *92*, 063302.

(25) Laudise, R. A.; Kloc, Ch.; Simpkins, P. G.; Siegrist, T. *J. Cryst. Growth* **1998**, *187*, 449.

(26) Jiang, L.; Gao, J.; Wang, E.; Li, H.; Wang, Z.; Hu, W.; Jiang, L. *Adv. Mater.* **2008**, *20*, 2735.

(27) Reese, C.; Roberts, M. E.; Parkin, S. R.; Bao, Z. *Appl. Phys. Lett.* **2009**, *94*, 202101.

(28) Lee, S. S.; Loth, M. A.; Anthony, J.; Loo, Y.-L. *J. Am. Chem. Soc.* **2012**, *134*, 5436.

DOI: 10.1021/jacs.5b01108
J. Am. Chem. Soc. 2015, 137, 12175−12178